Drop Formation and Control of Non-Newtonian Fluids

Z. Gao and K. Ng

Research Laboratories, Eastman Kodak Company, Rochester, NY, USA, zgao@kodak.com

ABSTRACT

It is well known that fluid jets tend to break up into droplets of multiple sizes. However, the ability to make and control individual droplets from arrays of such jets in speed, number, and size has become reality only recently in new generation Micro-Electro-Mechanical Systems (MEMS) technology. The talk will begin with an overview of MEMS-based microfluidic technology. The devices from this technology are capable of stimulating drop breakup of jets of complex fluids with unprecedented precision, speed, and selectivity. The instability of non-Newtonian liquid jets and drop formation from the MEMS-based microfluidic device is the main topic of the presentation. The governing equation for the surface profile of the liquid jet is derived in the forms of a partial differential equation (PDE). The PDE is solved for various cases of Carreau-Yasuda fluid to study the effect of fluid properties on jet breakup. The Carreau-Yasuda fluid has a power law viscosity bounded by an upper bound at zero strain rate and a lower bound at the infinite strain rate. The effects of various parameters on the instability behavior are studied in comparison with two Newtonian jets with upper and lower bound viscosities. A number of quantitative conclusions and sensitivities on the instability behavior of non-Newtonian jets are investigated. It is found that the jet breakup mechanism depends on the properties of the fluid as well as the wave number of the thermal disturbance that causes the surface tension gradient. In contrast to the Newtonian liquid, where the jet surface profile has the same frequency as the surface tension gradient, the nonlinear nature of the non-Newtonian constitutive behavior may tend to enable the jet surface profile at frequencies higher than that of the surface tension gradient. This leads to significant surface profile oscillation within one wavelength of the surface tension gradient and the generation of small satellite drops.

The present work can provide a good foundation for further investigations of the instability and breakup of non-Newtonian fluid jets under the situation where the surface tension gradient exits. The applications of such a phenomenon include microfluidic inkjet printheads with thousands of nozzles that are thermally modulated near the nozzle orifice to produce steady steams of picoliter-sized droplets at kilohertz frequency rates.

Keywords: *Jet breakup, Non-Newtonian fluid, Satellite drops, Jet stability, Inkjet.*

1. INTRODUCTION

The capillary instability of liquid jets has been the subject of numerous studies since the19th century when Lord Rayleigh considered the breakup of an inviscid cylindrical jet into drops [1]. However, the subject has been far from exhausted after more than several decades of scientific research, which in fact has gained considerable momentum in recent years. This is due partially to the fact that modern developments in the design and utilization of microfluidic devices for fluid transport have found many applications such as drug design and diagnostic devices in biomedicine and microdrop generators for image printing. Furthermore, the new development of nonlinear dynamics of the droplet has created a new paradigm of scaling and jet breakup that opened a new approach to this classic phenomenon. Currently, there is a considerable amount of literature available on Newtonian liquid jet instability. Some of the related references are reviewed in Gao [2]. However, things are more difficult for non-Newtonian jets caused by the complex nature of the constitutive behavior of such a liquid. Furthermore, relatively few authors have studied jet instability caused by spatial variations of surface tension, despite the practical relevance of this phenomenon [3,4]. In this paper, we discuss the drop formation and control of Non-Newtonian fluids driven by special variations of surface tension.

2. EQUATIONS

The governing equations for a jet of incompressible fluid, Figure 1, are the continuity equation and the momentum equation (ignoring gravity)

$$\nabla \cdot \boldsymbol{V} = 0 \tag{1}$$

$$\rho\left(\frac{\partial}{\partial t} + \boldsymbol{V}\cdot\nabla\right)\boldsymbol{V} = \nabla\cdot\boldsymbol{T} \tag{2}$$

where t is time, $\boldsymbol{V}$ is the jet velocity vector, $\boldsymbol{T}$ is the total stress tensor given as $\boldsymbol{T} = -p\boldsymbol{I} + \boldsymbol{t}$, where p is the pressure of the liquid, $\boldsymbol{t}$ is the stress tensor of the liquid, and $\boldsymbol{I}$ is the unit tensor. Also, $\boldsymbol{V} = (u, v)$ is the velocity, where u and v denote the radial and axial velocities, respectively. The stress tensor, which is given by $\boldsymbol{T} = -p\boldsymbol{I} + \mu(\dot{\gamma})[\nabla\boldsymbol{V} + (\nabla\boldsymbol{V})^T]$, where $\mu(\dot{\gamma})$ is the apparent viscosity function. The Carreau-Yasuda model

describing the deformation rate-dependent viscosity function (shear-thinning or shear-thickening) is

$$\mu(\dot{\gamma}) = (\mu_0 - \mu_\infty)(1 + |\beta\dot{\gamma}|^{\alpha})^{\frac{n-1}{\alpha}} + \mu_\infty \quad (3)$$

where

$$\dot{\gamma} = \left[2\left(\frac{\partial u}{\partial r}\right)^2 + \left(\frac{\partial u}{\partial z} + \frac{\partial v}{\partial r}\right)^2 + 2\left(\frac{\partial v}{\partial z}\right)^2 \right]^{1/2} \quad (4)$$

is the second invariant of rate-of-deformation tensor, and n is a power law exponent.

The Carreau-Yasuda model is one of the models used for describing the viscosity of a non-Newtonian fluid. Typically, based on the number of parameters, this is classified into three, four, and five parameter types, wherein the parameters, μ_∞, λ, and n are material coefficients, where, μ_∞ is the limiting viscosity at high shear stress, λ is a time constant calculated from the reciprocal of the strain rate at which the zero strain rate component and the power-law component of the flow curve intersect, and n is called Thixotropic index. The Thixotropic index is a ratio of a material's viscosity at two different speeds, generally different by a factor of ten. This index indicates the material's ability to hold its shape. The three-parameter model is called the Bird-Carreau model and the five-parameter model is the Carreau-Yasuda model. The power law model represents a shear-thinning fluid when $n < 1$, a shear- thickening fluid when $n > 1$, and a Newtonian fluid when $n = 1$. The Carreau-Yasuda model describes pseudoplastic flow with asymptotic viscosities at zero (μ_0) and infinite (μ_∞) shear rates, and with no yield stress. The parameter λ is a constant with units of time, where $1/\lambda$ is the critical shear rate at which viscosity begins to decrease. The power law slope is $(n - 1)$ and the parameter α represents the width of the transition region between μ_0 and the power law region. If μ_0 and μ_∞ are not known independently from the experiment, these quantities may be treated as additional adjustable parameters.

For a slender jet, Eq. (2) can be reduced to (see Gao and Ng [4] for details)

$$\frac{\partial v_0}{\partial t} + v_0\frac{\partial v_0}{\partial z} = -\frac{1}{\rho}\frac{\partial}{\partial z}(2\sigma H) + \frac{2}{\rho h}\frac{\partial \sigma}{\partial z} + \frac{3}{\rho h^2}\frac{\partial}{\partial z}\left(h^2\mu(z,t)\frac{\partial v_0}{\partial z}\right) \quad (5)$$

where v_0 is the leading term of the Taylor expansion with respect to r, of the axial velocity. The kinematic boundary condition requires that the fluid does not cross the free boundary, i.e.,

$$\frac{D}{Dt}(r - h) = 0, \text{ at } r = h, \quad (6)$$

which can be written as

$$\frac{\partial h}{\partial t} + v_z\frac{\partial h}{\partial z} = v_r, \text{ at } r = h. \quad (7)$$

The leading order equation that results from the kinematic boundary condition is

$$\frac{\partial h}{\partial t} + v_O\frac{\partial h}{\partial z} = -\frac{1}{2}h\frac{\partial v_0}{\partial z} \quad (8)$$

Let

$$v_0(z,t) = V_0 + v(z,t),\ h(z,t) = r_0\left[1 + \delta(z,t)\right]$$
$$\sigma(z,t) = \sigma_0 + \sigma_1(z,t)$$

where V_0, r_0, and σ_0 are the unperturbed velocity, radius, and surface tension of the jet, respectively, and v, δ and σ_1 are the perturbations. When we restrict to an analysis the purely temporal instability behavior of the jet (i.e., we do not consider traveling waves on the jet) and introduce a new variable $\eta = z - V_0 t$, Eqs. (5) and (8) become

$$\frac{\partial v}{\partial \eta} = -2\frac{\partial \delta}{\partial t} \quad (9)$$

$$\frac{\partial v}{\partial t} = \frac{\sigma_0}{\rho r_0}\left(\frac{\partial \delta}{\partial \eta} + r_0^2\frac{\partial^3 \delta}{\partial \eta^3}\right) + \frac{1}{\rho r_0}\frac{\partial \sigma_1}{\partial \eta} + \frac{3}{\rho}\frac{\partial}{\partial \eta}\left(\mu(\eta,t)\frac{\partial v}{\partial \eta}\right) \quad (10)$$

Using Eq. (9) to eliminate v from Eq. (10), we have a partial differential equation (PDE) for δ,

$$\frac{\partial^2 \delta}{\partial t^2} + \frac{\sigma_0}{2\rho r_0}\left[\frac{\partial^2 \delta}{\partial \eta^2} + r_0^2\frac{\partial^4 \delta}{\partial \eta^4}\right] - \frac{3}{\rho}\frac{\partial^2}{\partial \eta^2}\left[\mu(\eta,t)\frac{\partial \delta}{\partial t}\right] = -\frac{1}{2\rho r_0}\frac{\partial^2 \sigma_1}{\partial \eta^2} \quad (11)$$

Equation (11) is subjected to periodic boundary conditions and zero initial conditions

$$\delta(\eta, t = 0) = 0, \text{ and } \frac{\partial \delta}{\partial t}(\eta, t = 0) = 0 \text{ for all } \eta.$$

When a constitutive law for viscosity $\mu(\eta,t)$ is specified, Eq. (11) can be solved to determine the jet profile, δ, as a function of time. The jet breakup time is determined at the instance when δ is equal to -1. The

deformation rate defined in Eq. (4) can be further simplified as

$$\dot{\gamma} = [2(\frac{\partial v_r}{\partial r})^2 + 2(\frac{v_r}{r})^2 + (\frac{\partial v_r}{\partial z} + \frac{\partial v_z}{\partial r})^2 + 2(\frac{\partial v_z}{\partial z})^2]^{1/2}$$
$$= \sqrt{3(\frac{\partial v}{\partial z})^2} = \sqrt{3}\left|\frac{\partial v}{\partial z}\right| = 2\sqrt{3}\left|\frac{\partial \delta}{\partial t}\right|$$

Therefore, for the Carreau-Yasuda model shown in Eq. (3), we have

$$\mu(\eta,t) = (\mu_0 - \mu_\infty)[1 + |\beta\dot{\gamma}|^\alpha]^{\frac{n-1}{\alpha}} + \mu_\infty$$
$$= (\mu_0 - \mu_\infty)[1 + \left|2\sqrt{3}\beta\frac{\partial \delta}{\partial t}\right|^\alpha]^{\frac{n-1}{\alpha}} + \mu_\infty \quad (12)$$

Equation (11) may be further simplified to an ordinary differential equation (ODE) as shown below. Let

$$\sigma_1(\eta) = -\frac{\Delta\sigma}{2}\left[1 + \cos\left(\frac{\eta k}{r_0}\right)\right]$$
$$\delta(\eta,t) = y(t)\cos\left(\frac{\eta k}{r_0}\right) \quad (13)$$

Where $\Delta\sigma$ is the magnitude of the surface tension change along the jet, and *k* is the wave number. Equations (12) and (13) are substituted into Eq. (11); we have

$$\frac{d^2y(t)}{dt^2}\cos\left(\frac{\eta k}{r_0}\right) - \frac{\sigma_0}{2\rho r_0}\left(\frac{k}{r_0}\right)^2\left(1-k^2\right)y(t)\cos\left(\frac{\eta k}{r_0}\right)$$
$$-\frac{3}{\rho}\frac{\partial^2}{\partial\eta^2}\left\{\left[(\mu_0-\mu_\infty)\left(1+\left|2\sqrt{3}\lambda\frac{dy(t)}{dt}\cos\left(\frac{\eta k}{r_0}\right)\right|^\alpha\right)^{\frac{n-1}{\alpha}} + \mu_\infty\right]y(t)\cos\left(\frac{\eta k}{r_0}\right)\right\}$$
$$= \frac{\Delta\sigma}{4\rho r_0}\left(\frac{k}{r_0}\right)^2\cos\left(\frac{\eta k}{r_0}\right) \quad (14)$$

It is clear that because of the nonlinear nature of the Carreau-Yasuda model, the third term on the left-hand side of Eq. (14) involves power function of $\cos(\eta k/r_0)$. In the case of Newtonian flow, $n = 1$ and each term in Eq. (14) contains $\cos(\eta k/r_0)$. The term $\cos(\eta k/r_0)$ can be factored out to yield an ODE for $y(t)$. This is not the case when *n* is not equal to 1. However, if we focus our attention on the special region near the point where $\cos(\eta k/r_0)$ is close to 1, we can carry out the second-order derivatives with respect to η in the third term on the left-hand side of Eq. (14) and then let η approach to zero. Equation (14) is then reduced to an ODE for $y(t)$, subjected to the zero initial conditions $y(0) = y'(0) = 0$, where y' is the derivative of *y* with respect to *t:*

$$\frac{d^2y}{dt^2} + \frac{3}{\rho}\left(\frac{k}{r_0}\right)^2\left\{(\mu_0-\mu_\infty)\left[1+\left|2\sqrt{3}\lambda\frac{dy(t)}{dt}\right|^\alpha\right]^{\frac{-1-\alpha+n}{\alpha}}\left[1+n\left|2\sqrt{3}\lambda\frac{dy(t)}{dt}\right|^\alpha\right] + \mu_\infty\right\}\frac{dy(t)}{dt}$$
$$-\frac{\sigma_0}{2\rho r_0}\left(\frac{k}{r_0}\right)^2\left(1-k^2\right)y(t) = \frac{\Delta\sigma}{4\rho r_0}\left(\frac{k}{r_0}\right)^2 \quad (15)$$

In the following section, we will solve both the PDE (Eq. (11)) and the ODE (Eq. (15)) and compare the results for Newtonian and non-Newtonian fluids. It should be mentioned that the approximation of $\cos(\eta k/r_0)$ being close to 1 is not always justified. In such a case, the PDE in Eq. (11) should be used instead. More discussion will follow to show when such an assumption and the resulting ODE, Eq. (15), leads to results similar those from the PDE in Eq. (11).

3. RESULTS AND DISCUSSION

The surface tension defined in Eq. (13), is the driving force for the jet breakup. We demonstrate the model via application to a microjet of poly-Nisopropylacrylamide (poly-NIPAM) microgel solution. The properties are ρ = 1000 kgm^{-3}, r_0 = 5 μm, v_0 = 10 ms^{-1}, σ_0 = 0.073 N m^{-1}. At 2.5% concentration, n = 0.64, μ_0 = 0.026 N sm^{-2}, μ_∞ = 0.008 N sm^{-2}, λ = 0.2 s^{-1}, α = 1.4. The PDE for the perturbation of the radius of the microjet, Eq. (11), with periodic boundary conditions and zero initial conditions, is solved by the method of lines.

In Figure 1, the jet breakup time in microseconds is plotted as functions of wave number *k* for various values of *n*. In Figure 1, the dashed curve (called Carreau-PDE) and the dotted curve (called Carreau-ODE), are the breakup time for the PDE in Eq. (11) and the ODE in Eq. (15), respectively. The breakup times are obtained when $\delta(\eta,t) = -1$. The differences between the PDE and ODE breakup times are shown to be small. The solid curve in Figure 1, called Newtonian-μ_0, is from the breakup time of a Newtonian fluid with constant viscosity μ_0. Such curve is obtained with setting n = 1 for PDE (Eq. (11)) or ODE (Eq. (15)). The breakup time curve for such a Newtonian fluid has also been reported by Furlani [3]. The results from the present paper match exactly those from Furlani [3] for the Newtonian fluids (with constant viscosity at μ_0 and μ_∞). The upper bound breakup time is from the Newtonian fluid with constant viscosity μ_0 and the lower bound breakup time is from the Newtonian fluid with constant viscosity μ_∞ (the dashed-dotted curve, called Newtonian-μ_∞). Note that the Carreau-Yasuda fluid has a viscosity bounded by μ_0 and μ_∞, i.e., $\mu_\infty < \mu \le \mu_0$. It

seems to be logical that the breakup times for Carreau-Yasuda fluid are bounded by Newtonian-μ_∞ and Newtonian-μ_0.

The relative positions of the breakup time curve for the PDE and the ODE to the upper and lower bound Newtonian curves depend on the parameter *n*. For example, when *n* is 0.64, the PDE and ODE curves move very close to the Newtonian-μ_∞ curve. The reason is that as we reduce *n* from 0.9 to 0.64, the viscosity as a function of strain rate reduces its value from μ_0 to μ_∞ much faster. Therefore, the jet breakup behavior is dominated to a larger extent by μ_∞. When the value of the parameter *n* is changed to 0.99, the viscosity of the Carreau-Yasuda fluid approach to μ_∞ is much slower. Therefore, the jet breakup is dominated by the viscosity of the Carreau-Yasuda fluid at low strain rate. As we can see from Figure 1, both PDE and ODE breakup time curves (Carreau-PDE and Carreau-ODE) are very close to that for a Newtonian fluid with μ_0. However, the solution for Carreau-PDE for *k* less than 0.2 is below the breakup time curve for Newtonian fluid with μ_∞ (Newtonian-μ_∞). This appears to be an anomaly since the viscosity of the Carreau-Yasuda fluid has a viscosity that is always higher than μ_∞.

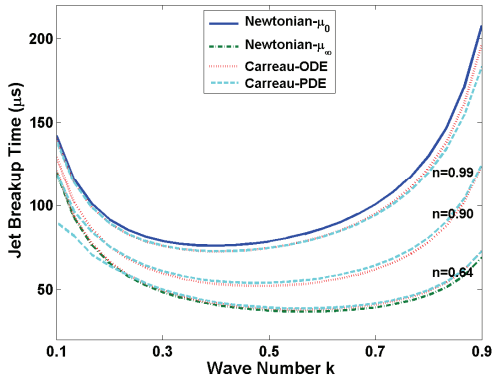

Figure 1. The breakup time versus wave number for Newtonian and Carreau-Yasuda fluid for various values of *n*.

Figure 2 shows jet profile for three solutions (Carreau-PDE, Newtonian - μ_0, and Newtonian - μ_∞) at the instance when the Carreau-PDE solution yields the jet breakup. The wave number *k* is equal to 0.1, and *n* is equal to 0.64. Two things are important to notice. First, the jet break point is not at the $\eta = 0$ as the case for a Newtonian fluid. Secondly, the jet profile for the Carreau-Yasuda fluid shows significant oscillations (higher frequencies than that of the surface tension gradient). We postulate that the spatial variation of the viscosity in the jet further enhances the velocity variation in the jet that causes significant oscillations of the jet. This leads to an early jet breakup for the Carreau-Yasuda fluid, even earlier than one Newtonian fluid with a lower viscosity, μ_∞. Figure 3 is a plot showing the profile of a Carreau-Yasuda fluid obtained by the PDE solution at breakup for two wavelengths. Instead of two drops, as in the case of a Newtonian fluid at breakup, the figure clearly shows the formation of satellite drops. The control of satellite drops is important for many microfluidic applications such as inkjet printing.

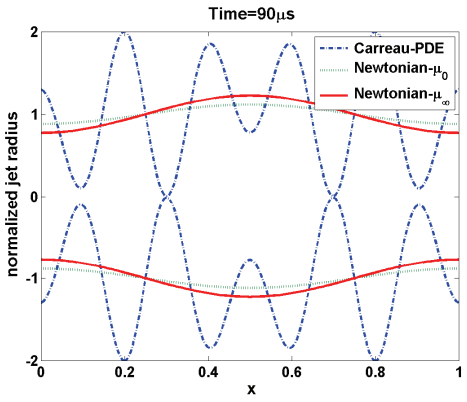

Figure 2. The normalized jet profiles for Newtonian and Carreau-Yasuda fluids at jet breakup when the wave number k = 0.1

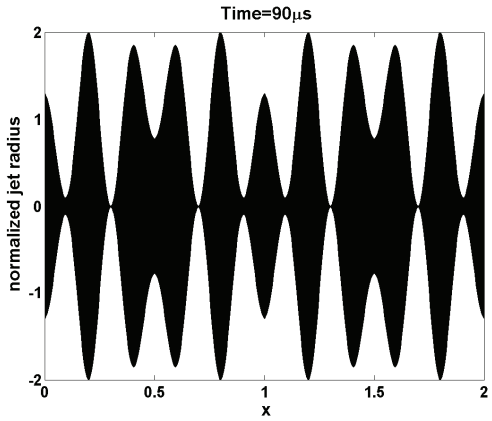

Figure 3. The normalized jet profiles for Carreau-Yasuda fluid at breakup (t = 90 μs) for two wavelength. Satellite drops are formed.

REFERENCES

[1] Rayleigh Lord 1878 On the Instability of Jets, *Proc. London, Math. Soc. X.*

[2] Gao Z. Instability of non-Newtonian jets with a surface tension gradient. *J. Phys A: Math Theor* 2009;42.

[3] Furlani E P 2005 Temporal instability of viscous liquid microjets with spatially varying surface tension *J. Phys. A: Math. Gen.* **38** 263–276.

[4] Gao Z and Ng K. Temporal analysis of power law liquid jets, *Computers & Fluids* **39** (2010) 820–828.